Influence of absorber doping in a-SiC:H/a-Si:H/a-SiGe:H solar cells

Muhammad Nawaz[1, †] and Ashfaq Ahmad[2]

[1]University Graduate Centre (UNIK), Gunnar Randers Vei 19, P. O. Box 70, N-2027 Kjeller, Norway
[2]COMSATs Institute of Information Technology, Off-Raiwand Road, Lahore-54000, Pakistan

Abstract: This work deals with the design evaluation and influence of absorber doping for a-Si:H/a-SiC:H/a-SiGe:H based thin-film solar cells using a two-dimensional computer aided design (TCAD) tool. Various physical parameters of the layered structure, such as doping and thickness of the absorber layer, have been studied. For reliable device simulation with realistic predictability, the device performance is evaluated by implementing necessary models (e.g., surface recombinations, thermionic field emission tunneling model for carrier transport at the heterojunction, Schokley–Read Hall recombination model, Auger recombination model, bandgap narrowing effects, doping and temperature dependent mobility model and using Fermi–Dirac statistics). A single absorber with a graded design gives an efficiency of 10.1% for 800 nm thick multiband absorption. Similarly, a tandem design shows an efficiency of 10.4% with a total absorber of thickness of 800 nm at a bandgap of 1.75 eV and 1.0 eV for the top a-Si and bottom a-SiGe component cells. A moderate n-doping in the absorber helps to improve the efficiency while p doping in the absorber degrades efficiency due to a decrease in the V_{OC} (and fill factor) of the device.

Key words: solar cells; modeling; TCAD; amorphous silicon; HIT cells
DOI: 10.1088/1674-4926/33/4/042001 **EEACC:** 2520

1. Introduction

Thin-film amorphous silicon (and their alloys) based solar cells[1−7] provide the best cost reduction alternative for photovoltaic modules due to less silicon consumption and a stable efficiency performance due to the reduced absorber thickness after light soaking. The use of bandgap engineering in amorphous a silicon network (i.e., a-Si, a-SiGe, a-SiC) presents itself as a promising opportunity to optimize efficiency in thin-film solar cells. Primarily, the application of a-Si:H based solar cells offer four advantages: first, the simple fabrication of a-Si:H (and their alloys) films by the decomposition of silane (SiH_4) using PECVD system; second, the high absorption coefficient (α) of the a-Si:H material resulting in low material consumption; third, the amorphous material can be deposited on different substrates that can withstand the process temperature of 250–300 ℃; fourth, the a-Si:H solar cells can be fabricated in a continuous process as integrated solar modules. The incorporation of Ge and C into the amorphous a-Si:H material, principally opens up a bandgap of 1–3 eV for solar cell applications (a range of 1.5–2.2 eV is effectively used today) that results in a significant optimization of the absorption profile. In addition, the generation of an additional built-in electric field profile or the establishment of diffusion barriers for charge carriers can be achieved. Note that thin amorphous hydrogenated silicon carbide (a-SiC:H) films are widely used as active window layers to enhance optical transparency by widening the bandgap of the material. Hydrogenated amorphous silicon germanium (a-SiGe:H) is often used as the absorber material in tandem cell configurations since the red response of a-SiGe:H subcell is higher as compared to an a-Si:H cell.

In pin (superstrate) or nip (substrate) type a-Si solar cells, the intrinsic absorber layer is sandwiched between the p and n a-Si layers and the absorber layer is left usually undoped (intrinsic). Earlier reports have indicated the presence of unintentional background impurities (e.g., oxygen, nitrogen, fluorine, etc) in the a-Si absorber layer[2, 3] and decay of efficiency has been linked with these impurities. Some experimental work[4, 6] has also reported the influence of n-type and p-type doping (i.e., P and B) in the absorber layer on the carrier collection efficiency in a-Si pin solar cells. The main objective in this paper is to understand and quantify the mechanism behind the efficiency enhancement (observed in present numerical simulation) due to limited n-type doping presence in the absorber layer, while the p-type doping in the absorber has been found to be counterproductive from the point of view of efficiency.

2. Device simulation setup

The details of the layer structures studied in this analysis are shown in Fig. 1. A two-dimensional numerical simulation (TCAD from Silvaco[8]) analysis of the single-junction absorbers of various bandgap materials is shown in Fig. 1(a) and a double junction tandem design using top a-Si component cell and bottom a-SiGe component cell (Fig. 1(b)) is reported. The device performance is evaluated by implementing special models (e.g., surface recombination, interface traps, thermionic field emission tunneling model for carrier transport at the heterojunction, etc) at the semiconductor-semiconductor interface and semiconductor–metal interfaces. The simulation is based on the implementation of Schokley–Read Hall recombination, Auger recombination, bandgap narrowing effects, doping and temperature dependent mobility model and using Fermi–Dirac statistics. The numerical simulation is composed

† Corresponding author. Email: nawaz@unik.no
Received 2 October 2011

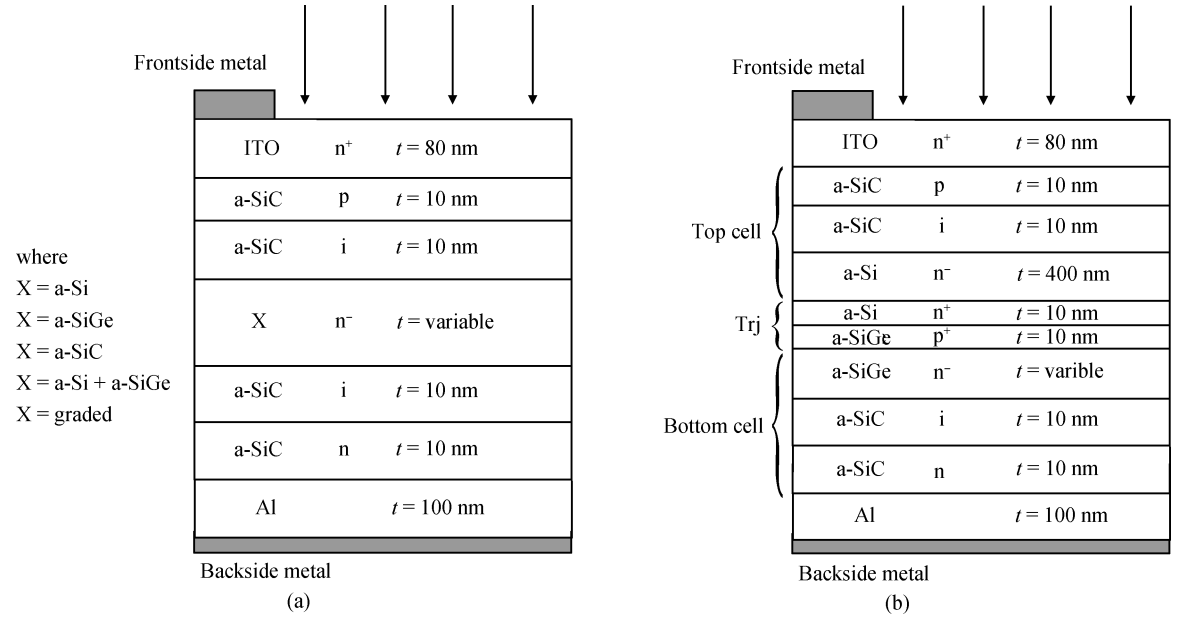

Fig. 1. A schematic view of simulated layer structures with (a) single absorber X and (b) tandem design in n–i–p configuration.

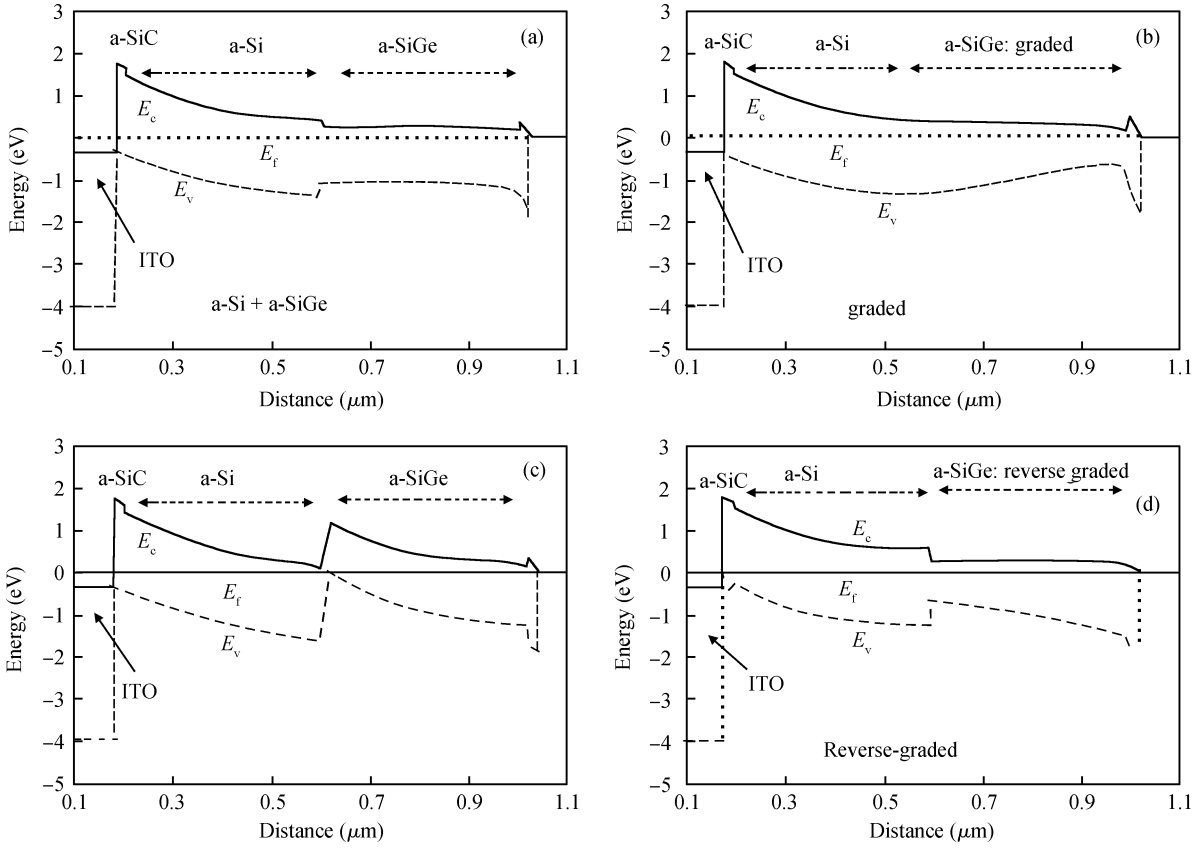

Fig. 2. Energy band diagram in equilibrium for four design approaches namely for (a) combined a-Si + a-SiGe absorber, (b) graded a-SiGe absorber, (c) tandem design, and (d) reverse-graded a-SiGe absorber.

of 38000 mesh points with a fine mesh resolution of 0.2 nm close to the heterointerfaces. The simulation data deals with the AM1.5 solar spectrum at room temperature. Nominal bandgaps of 3.7, 1.75, 1.95 and 1.39 eV have been used for ITO, a-Si:H, a-SiC:H and a-SiGe:H material, respectively. An affinity value of 4.5, 4.03, 3.95 and 1.39 eV has been set for ITO, a-Si:H, a-SiC:H and a-SiGe:H material, respectively. Similarly, the electron and hole lifetime has been fixed at 1 μs for each amorphous material. Electron (hole) mobility for ITO material has been chosen to be 60 (20) cm^2/(V·s) for ITO material, while the electron (hole) mobility value of the amorphous Si network has been kept same at 10 (2) cm^2/(V·s). The effective density

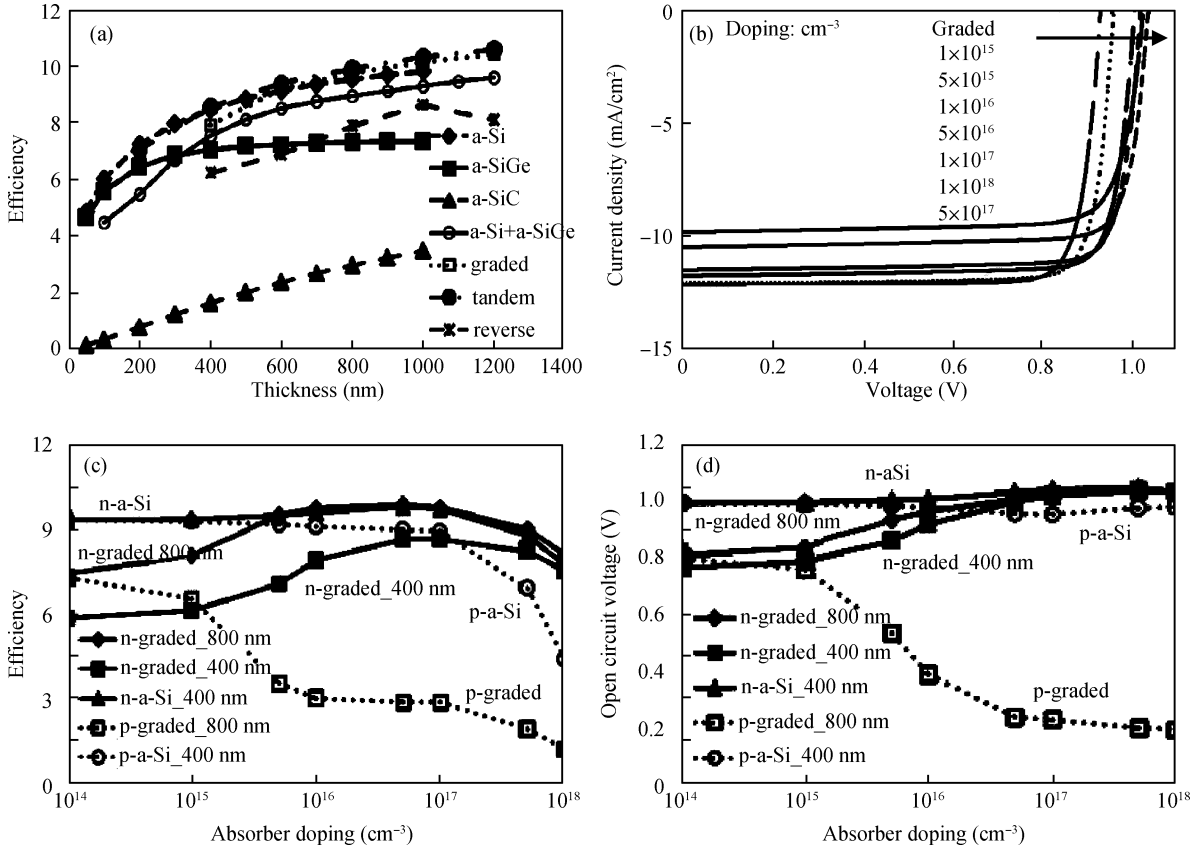

Fig. 3. (a) Efficiency versus absorber thickness for various design and (b) current–voltage characteristics for single absorber of graded profile with various n-doping in the absorber layer. Also shown is (c) the efficiency and (d) open circuit voltage V_{OC} as a function of absorber doping. Nominal bandgap of a-Si is 1.75 eV, a-SiGe is 1.39 eV and a-SiC is 1.95 eV.

of state in the conduction band (valence band) of the amorphous silicon network is set to 2.5×10^{20} (2.5×10^{20}) cm^{-3}. Similarly, the conduction (valence) band tail energy of a-Si:H (and their alloys) has been fixed at 22 (55) meV. Finally, the Gaussian defect density in the bandgap is also kept constant at 1×10^{15} cm^{-3} for a-Si (and their alloys). Details of the defect density distribution are given elsewhere[7].

The modeling details (refractive indexes, absorption coefficient, etc) of these structures are given elsewhere[7]. A graded design in nip type configuration has a total absorber thickness of 800 nm (i.e., 400 nm of a-Si top absorber portion and 400 nm of a-SiGe bottom absorber portion) and grading was employed (in steps of 50 nm for each bandgap) only at the lower part of the a-SiGe absorber from 1.5 to 0.9 eV (in decreasing bandgap values from top to bottom and increasing bandgap values for reverse-graded design). The energy band diagram of various design approaches (i.e., combined a-Si + a-SiGe absorber (Fig. 2(a)), graded aSiGe absorber design (Fig. 2(b)), tandem design with top a-Si component cell and bottom a-SiGe component cell (Fig. 2(c)), and reverse-graded aSiGe absorber (Fig. 2(d)) is shown in Fig. 2.

3. Results and discussion

Efficiency versus intrinsic absorber layer thickness for various design approaches is shown in Fig. 3(a). The results are shown for a single junction absorber of a-Si, a-SiGe, a-SiC, combined a-Si + a-SiGe and graded absorber with a top a-Si ($E_g = 1.75$ eV) layer and a bottom graded a-SiGe region. In the graded design, the total thickness of the intrinsic absorber was the sum of the single a-Si layer and multiple a-SiGe layers. Note that the grading was only employed in the bottom portion of the a-SiGe absorber with decreasing bandgap (with E_g from 1.6 to 0.9 eV) towards the bottom of the device. Efficiency data of tandem (tdm) type design is based on the amorphous silicon network with a top a-Si ($E_g = 1.75$ eV) component cell and a bottom component cell of a-SiGe ($E_g = 1.39$ eV). In general, efficiency increases with the increase of the absorber thickness (Fig. 3(a)) as expected due to increase in the short circuit current. Efficiency starts saturating once absorber layer thickness reaches around 700 nm. Out of various single junction absorbers (i.e., a-Si, a-SiGe, a-SiC, a-Si + a-SiGe, graded and reverse-graded), the graded design shows better efficiency performance for thick absorber layers (i.e., > 600 nm) as this allows better utilization of the solar spectrum of longer wavelength photons. For combined absorber material (i.e., a-Si + a-SiGe), the absorber is set to equal thickness with a bandgap of 1.75 eV for a-Si and 1.39 eV for a-SiGe. For the graded design, the absorber is composed of a top a-Si part (1.75 eV) and a bottom graded part of a-SiGe with grading from 1.60 to 0.9 eV. The reverse-graded design shows weak efficiency performance due to appearance of a potential barrier at the interface of the a-Si top portion and the a-SiGe bottom portion of the absorber (Fig. 2(d)). Thus, photogenerated holes in the bottom graded a-SiGe sides cannot reach to top side of the device, which results in a lower value of efficiency. Overall, the

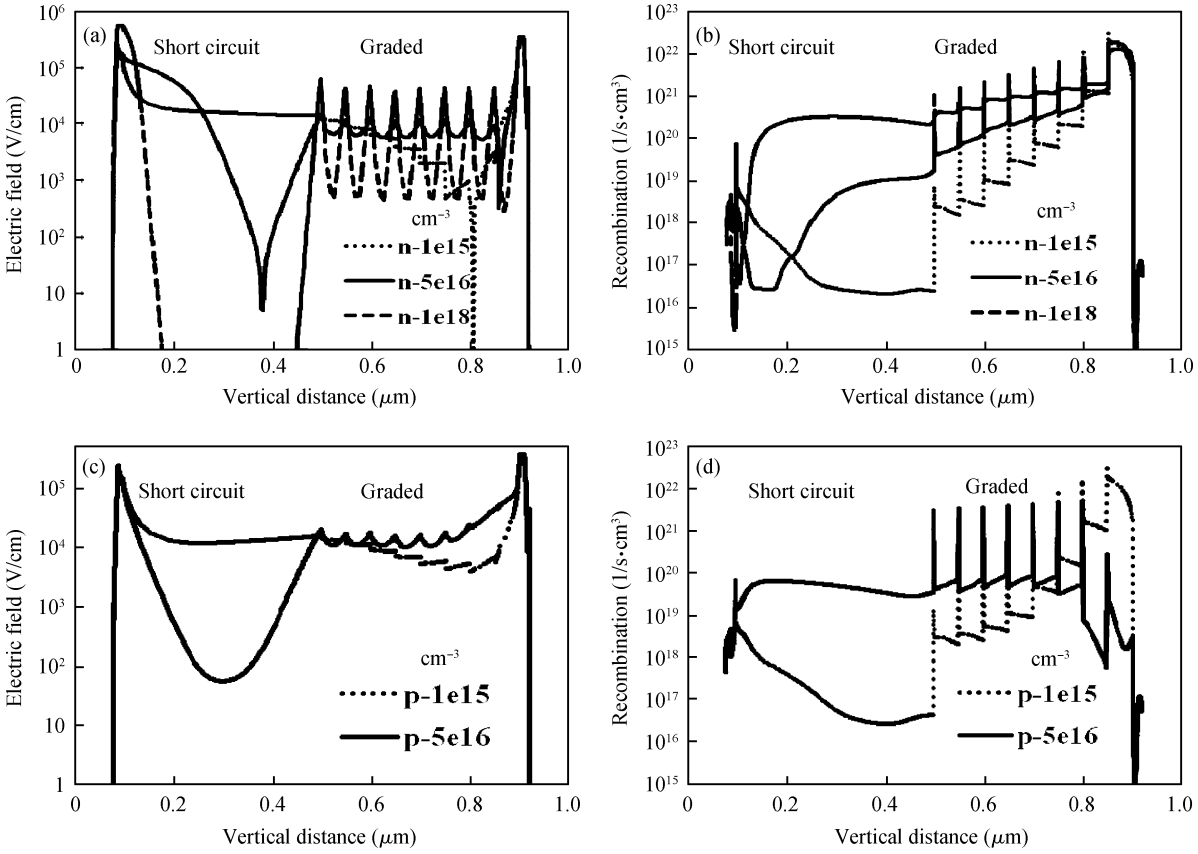

Fig. 4. (a, c) Electric field and (b, d) recombination rate profiles as a function of vertical depth for a graded single junction absorber under short circuit conditions for different (a, b) n-type and (c, d) p-type absorber doping.

tandem (tdm) cell design shows the best conversion efficiency exceeding 10%. The single junction absorber based on only a-SiGe material has a predicted maximum efficiency of just 7%. Similarly, the efficiency of a single junction absorber based on a-SiC material is just over 3% (due to a very low absorption coefficient[7]) for the thickness range studied. With comparable efficiency performance, a single absorber with a graded design approach is still the better choice since it avoids the current matching critically needed in tandem designs without optimizing the thin high doped tunnel recombination junction between the two cells. Furthermore, the single absorber design with a graded profile also facilitates carrier transport (additional built-in electric field), which is rather smooth where the carriers are collected at the respective contacts without the hindrance of any potential barrier (hence better collection efficiency). One possible disadvantage with the choice of graded design is that the quality of the material degrades when more Ge is incorporated into the film for reducing the bandgap of a-SiGe material, indicating that the grading is only applicable to a limited range of bandgap values.

The influence of n and p-type absorber doping on efficiency for 400 nm and 800 nm thick absorbers is also shown in Figs. 3(b)–3(d) for a single absorber of graded design and for a single bandgap a-Si (1.75 eV) absorber. Efficiency increases at first with the increase of n-doping in the absorber, reaches a maximum value and then decreases with a further increase in the n-doping both for the 400 and the 800 nm thick absorbers. Following the introduction of p-type doping in the absorber, efficiency decreases continuously with the increase of p-doping both for single bandgap (a-Si) and graded absorber designs. Figure 4 illustrates the electric field and recombination rate profiles as a function of vertical depth for a graded single junction absorber under short circuit conditions for different n-type and p-type absorber dopings. The results are explained by using a modified electric field profile and the change in the recombination rate (Fig. 4) within the absorber induced by the variation in doping. The appearance of peaks and valleys in the electric field and the recombination rate profile of the graded design at the bottom side of the absorber is due to the potential variation at the graded interfaces of the region. Looking first at the p-doped absorber (Figs. 4(c) and 4(d)), the field drops significantly in the top portion of the absorber with higher p-doping (p: 5×10^{16} cm^{-3}) and remains at higher values ($\sim$10 kV/cm) at the bottom side of the absorber. Thus, photogenerated carriers in the top portion are not supported by the very low field while holes (i.e., heavy and with low mobility) generated at the lower side of the absorber and they cannot pass through the low field zone either. This leads to a higher np product and hence a higher overall recombination rate in the whole absorber (Fig. 4(d)) with a larger p-doping presence. So, accordingly, a significant drop in efficiency occurs with higher p-doping, which is consistent with the decrease in the V_{OC} (Fig. 3(d)) and fill factor. Figure 5 shows the electric field and recombination rate profiles as a function of vertical depth for a graded single junction absorber under open circuit conditions, and a conventional a-Si pin type absorber under short circuit conditions for

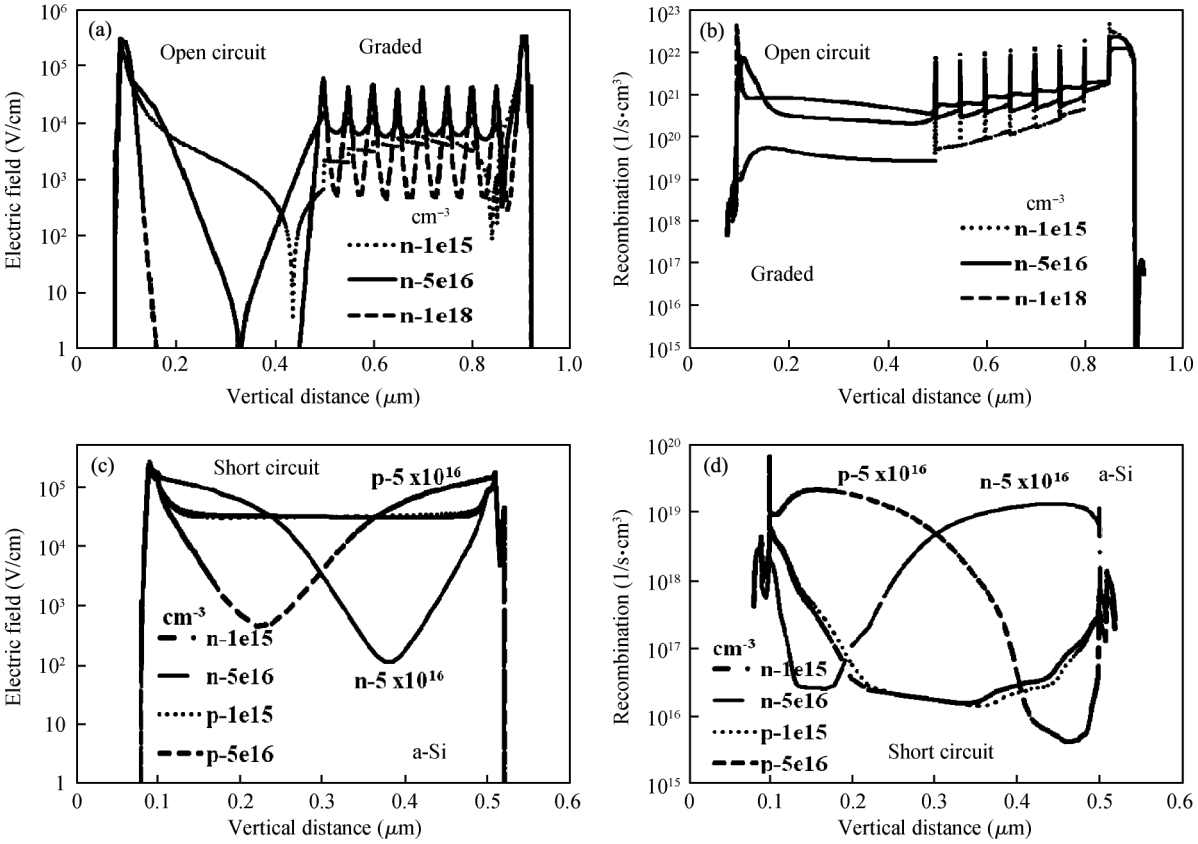

Fig. 5. (a, c) Electric field and (b, d) recombination rate profiles as a function of vertical depth for (a, b) graded single junction absorber under open circuit conditions and (c, d) conventional a-Si pin type absorber under short circuit conditions for different n-type and p-type absorber doping.

different n-type and p-type absorber dopings. For a-Si absorber design, the field is uniform at low n or p doping (Fig. 5(c)) in the absorber. The field drops to a lower value at the top side of the absorber if it is doped to p-type and drops at the bottom side if it is doped to n-type. This doping induced change in the field is also reflected in the recombination rate profile (Fig. 5(d)) of the a-Si absorber design.

The situation is different with n-doping (Figs. 4(a), 4(b)) in the graded absorber. Compared to lower n-doping (1×10^{15} cm^{-3}), the field is higher over an extended portion of the top side of the absorber, and over the bottom side of the absorber with moderately higher n-doping. This leads to an improved collection efficiency for photogenerated holes in the top absorber portion (higher electric field over larger drift length) and photogenerated electrons in the bottom side of the absorber. While a slight decrease in the short circuit current density is noticed (Fig. 3(b)), the rate of increase of V_{OC} (and V_m and hence fill factor) is larger with an initial increase in n-doping in the graded absorber. This leads to a higher efficiency initially with the increase in doping. For very large n-doping (1×10^{18} cm^{-3}), the field drops rapidly over a larger portion of the absorber and does not support the photogenerated carrier collection. This is also reflected in the increased overall recombination rate due to the presence of a large amount of photogenerated carriers in the whole absorber for very large doping. As a result, the electron and hole current densities decrease with higher doping, as is noticed in the simulation. So, the net effect of doping induced change in the electric field and recombination leads to a small decrease in the J_{SC} and a faster increase in the V_{OC} (overall higher field over larger drift length in the absorber) with an initial increase in the doping up to 5×10^{16} cm^{-3}. Hence, an increase in the solar cell efficiency from 8.05 to 9.87% is expected with doping variation from 1×10^{15} to 5×10^{16} cm^{-3}. Overall, the field variation in the top portion of the absorber is more doping sensitive as compared to the bottom graded side of the absorber.

Note that the double heterojunction structure is composed of p^+/n^- (top side: major junction) and n^-/n^+ (bottom side: minor junction), and the built-in potential in the cell splits asymmetrically between the top and bottom heterojunction regions. So, a slight change in the n-doping in the absorber may result in a pronounced change in the built-in potential at the top heterojunction. V_{OC} is primarily determined by the built in potential of the p^+/n^- major junction and is less sensitive to n^-/n^+ side where a smaller variation in electric field is observed with n-doping. The results of the influence of doping dependent efficiency behavior presented here are fairly consistent with earlier simple calculations for thin-a-Si solar cells[9, 10].

4. Conclusion

Two-dimensional numerical simulations of thin film a-Si:H solar cells predict an efficiency of over 10% for a single junction absorber with an a-SiGe graded profile at the bottom side of the absorber region. A moderate n-doping ($1–5 \times 10^{16}$ cm^{-3}) in the absorber further helps to improve the ef-

ficiency, while p-doping in the absorber is counterproductive because efficiency degrades with the increase of p-doping. Numerical simulations predict that this efficiency performance is only guaranteed if the defect density in the a-Si network lies in the range of $0.1–5 \times 10^{16}$ cm^{-3}.

References

[1] Yang J, Banerjee A, Guha S. Amorphous silicon based photovoltaics—from earth to the final frontier. Solar Energy Materials & Solar Cells, 2003, 78: 597

[2] Ganguly G, Carlson D E. Sensitivity of amorphous silicon-germanium solar cells to oxygen impurity atoms. Appl Phys Lett, 2003, 83(4): 683

[3] Woerdenweber J, Merdzhanova T, Stiebig H, et al. Critical oxygen concentration in hydrogenated amorphous silicon solar cells dependent on the contamination source. Appl Phys Lett, 2010, 96(10): 103505

[4] Kondo M, Nishio H, Yamagishi H, et al. Effects of low level doping of i-layer in a-SiC:H/a-Si:H heterojunction solar cells. Proc 19th IEEE Photovoltaic Specialist Conference, New Orleans, 1987: 604

[5] Sakai H, Kamiyama M, Uchida Y, et al. Carrier collection enhancement by boron doping in the i-layer of pin a-Si:H solar cell. J Non-Crystalline Solids, 1983, 59/60, Part 2: 1151

[6] Haruki H, Sakai H, Kamiyama M, et al. Effect of boron doping and its profile on characteristics of p–i–n a-Si: solar cells. Solar Energy Mater, 1983, 8(4): 441

[7] Nawaz M. Computer analysis of thin-film amorphous heterojunction solar cells. J Phys D, 2011, 44: 145105

[8] Silvaco Data System Inc, Atlas User Manual Ver 5.15.31.C, 2009

[9] Prentice J. Computer simulation of the effect of phosphorus doping of the i-layer in a thin film a-Si:H p–i–n solar cell. Solar Energy Materials and Solar Cells, 2000, 61: 287

[10] Pawlikiewicz A H, Guha S. The effect of dominant junction on the open circuit voltage of amorphous alloy solar cells. Mat Res Soc Symp Proc, 1988, 118: 599